Biobased monomers · Enzymatic polymerization · Furan-based copolyesters

Enzymatically catalyzed furan-based copolyesters containing dimerized fatty acid derivative as a building block

Martyna Sokołowska[1], Jagoda Nowak-Grzebyta[2], Ewa Stachowska[2], Piotr Miądlicki[3], Beata Michalkiewicz[3], Miroslawa El Fray[1*]

[1]West Pomeranian University of Technology, Szczecin, Faculty of Chemical Technology and Engineering, Department of Polymer and Biomaterials Science, Al. Piastow 45, 71-311 Szczecin, Poland

[2]Poznan University of Technology, Faculty of Mechanical Engineering, ul. Piotrowo 3, 60-965 Poznan, Poland

[3]West Pomeranian University of Technology, Szczecin, Faculty of Chemical Technology and Engineering, Engineering of Catalytic and Sorbent Materials Department, Al. Piastow 45, 71-311 Szczecin, Poland

*Corresponding author: mirfray@zut.edu.pl

Abstract

An environmentally friendly method of creating sustainable alternatives to traditional aromatic-aliphatic polyesters is discussed as a valuable step towards resource-efficiency optimization. A group of furan-based copolymers was synthesised via temperature-varied two-step polycondensation reaction in diphenyl ether using *Candida antarctica* lipase B (CAL-B) as biocatalyst where dimethyl 2,5-furandicarboxylate (DMFDCA), α,ω-aliphatic linear diols (α,ω-ALD), and dimerized fatty acid diol (DLD) were used as the starting materials. Nuclear magnetic spectroscopy (^{1}H and ^{13}C NMR), Fourier transform spectroscopy (FTIR) and gel permeation chromatography (GPC) were used to analyze the resulting copolymers. Additionally, crystallization behavior and thermal properties were studied using X-ray diffraction (XRD), digital holographic microscopy (DHM), and differential scanning

microscopy (DSC). The results showed that the diol chain length of α,ω-ALD used in the synthesis had a significant effect on the material thermal properties and crystalline structure thus being an important guideline in design of entirely bio-based copolymers prepared by biocatalytic process.

1. Introduction

Nowadays, cumulative environmental pollution, greenhouse gas emissions, and climate change are leading to the development of new ideas and solutions which need to be implemented to reduce the undesirable effects caused by the processing of fossil resources [1,2]. Therefore, the use of biomass as a raw material for the production of chemicals has been a focus for many years as concerns over the sustainability of chemical manufacturing have become increasingly important. Currently, one of the research activities is heavily focused on replacing terephthalic acid (TPA) with 2,5-furandicarboxylic acid (FDCA) since it possesses a similar chemical structure and can be fully obtained from renewable resources via oxidative conversion of 5-hydroxymethylfurfural (HMF) produced by acidic dehydrogenation of hexoses (Fig. 1). It is reflected by many published papers and approaches which are describing the use of FDCA with various monomers in polymer synthesis [3–12]. To be more precise, great attention is dedicated to the development of semicrystalline polyesters and copolyesters since they exhibit several advantageous features and prevalent usability as engineering, packaging, textile, and elastomeric materials [13,14]. One of the materials that present special potential as biobased alternatives for TPA-based polymers such as: poly(ethylene terephthalate) (PET) or poly(butylene terephthalate) (PBT) are poly(ethylene furanoate) (PEF) and poly(butylene furanoate) (PBF), whereas PEF is already produced at pilot scale and used in commercial applications as packaging material for soft drinks, films, and fibers [15]. These semicrystalline engineering thermoplastics exhibit similar and even better mechanical properties, increased chemical and thermal stability, electrical insulation, excellent barrier properties, and higher ability of polymer chain orientation compared to its TPA-based analogs [16,17]. For example, Papageorgiou *et al.* [10,18] analyzed in detail the phase transitions and crystal structure of 2,5-FDCA-based and TPA-based polyesters. The obtained results suggest that barrier properties against oxygen, carbon dioxide, and water vapor were significantly improved in the case of 2,5-FDCA analog compared to PET, what means that these materials could be suitable for food packaging applications. Moreover, based on Knoop and co-workers [19], the mechanical properties of 2,5-FDCA polyesters are comparable to those of PET. On the other hand, Jing *et al.* showed that polyesters obtained via polycondensation of 2,5-FDCA with ethylene glycol (EG), propylene glycol (PG), and butylene glycol (BG) possess a lower melting temperature, higher glass transition temperature, and slightly lower thermal stability in comparison to TPA-based counterparts [12]. These results also revealed that all polymers are semicrystalline materials but crystallize slower than polyesters possessing a benzene ring and these features are beneficial from a processing point of view, as the lower melting temperature combined with

still high heat resistance facilitates the film blowing and extrusion processes which directly translate to lower energy consumption.
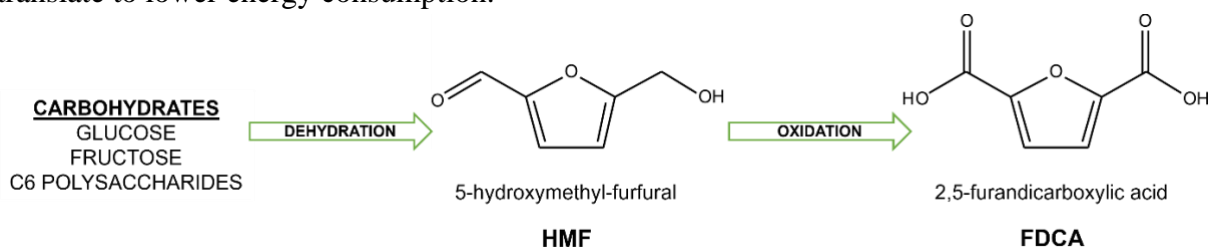
Figure 1. General procedure to produce HMF and FDCA from hexoses and C6 polysaccharides.

It is undeniable, that above mentioned furan-based polyesters are characterized by outstanding and promising properties, however, their synthesis is usually performed using metal catalysts at a high temperature above 200 °C. At that temperature range FDCA can undergo decomposition or side reactions which may lead to material discoloration [20]. Therefore, there is a need to search for a new catalytic system that will enable to perform synthesis in lower temperatures and replace rather toxic tetrabutyl titanate or Sb_3O_4 whose residues may remain in the material after synthesis and be harmful to the environment. Thus, to contribute to the principles of sustainable development of polymers by using renewable raw materials, it is necessary to also think about catalysts to create an entirely eco-friendly pathway for furan-based polyester production.

Enzymes are an interesting alternative as nature's catalysts which has a chance to replace conventional techniques and physical modification methods [21]. They exhibit a number of advantages, including high efficiency, substrate specificity, catalyst recyclability, and the ability to work under mild reaction conditions [22]. Lipases are the most widely employed enzymes in organic reactions such as transesterification, esterification, aminolysis, and Michel addition [23]. *Candida antarctica* lipase B (CAL-B) is a good catalyst for these reactions because of its stability and high reactivity. Moreover, the unique structure of CAL-B active site pocket is responsible for the high regio-, enantio-, and stereoselectivity of this enzyme due to which it is possible to obtain materials with a well-defined chemical structure which is a desirable feature e.g. in the pharmaceutical industry [24]. We also confirmed this fact in our previous work [25] where the poly(butylene succinate)-based copolyesters obtained with the use of CAL-B were characterized by a more regular structure compared to the materials synthesized using a metal catalyst. Notably, besides succinate-based polyesters [26,27], many types of other polymers have been successfully synthesized *via* CAL-B-catalyzed polymerization, including polyesters such as 2,5-furandicarboxylic acid-based polyesters [9,11], vegetal oil-based polyesters [28], sugar-based polyesters [29], and 3,6-dianhydrohexitol-based polyesters [30]. It is also noteworthy that the immobilized form of CAL-B can be conveniently removed from the reaction mixture through filtration, unlike metal catalysts which are prone to strong metal-metal interactions and often remain in the final product, making removal difficult. This makes enzymatic catalysts a more desirable option for resource-efficient and optimized synthesis processes.

Dimerization of fatty acids mainly C18 vegetable unsaturated fatty acids like oleic or linoleic acid is triggering increasing attention in sustainable polymer chemistry. Subsequent

hydrogenation or reduction of C18 fatty acids yields difunctional monomers: fatty dimer diols or fatty dimer acids characterized by low glass transition temperature, amorphous structure, and high conformational flexibility of aliphatic chains. They are attractive biobased components to create soft segments within copolyesters and it was also proved in our previous studies where enzymatic synthesis of poly(butylene succinate)-co-(dilinoleic succinate) multiblock copolyesters was performed where dilinoleic diol (DLD) was used as a building block to create soft segments [25,31]. Additionally, a recent study of Kwiatkowska *et al.* demonstrated the synthesis of 2,5–poly(butylene furanoate) with variable content of DLD indicating successful direct esterification of FDCA with 1,3–propanediol and subsequent copolymerization with DLD [6].

Therefore, the idea of this work is to expand the range of polyester materials that can be synthesized from renewable resources using CAL-B as a biocatalyst and also to deliver the detailed characteristic of new furan-based block copolyesters. Moreover, in this paper, we will investigate how the chain length of diols (C = 6, 8, 10, 12) used to form hard segments are influencing the synthesis efficiency, crystalline structure, and thermal properties. Findings of this research have the potential to contribute to the development of more environmentally friendly and sustainable polymeric materials, thereby influencing resource-efficiency optimization in the field of polymer science.

2. Materials and Methods

2.1 Materials

The following chemicals were bought from Sigma-Aldrich (Poznan, Poland): 1,6-hexanediol (1,6-HDO; ≥99%), 1,12-dodecanediol (1,12-DDDO; ≥99%), diphenyl ether (DE; ≥99%). 1,8-octanediol (ODO; ≥98%), and 1,10-decanediol (DDO; ≥99%) were acquired from Acros Organics (Geel, Belgium). Dimethyl 2,5-furandicarboxylate (2,5-DMFDCA; ≥99%) was obtained from Fluorochem (Lodz, Poland). Dimer linoleic diol (DLD; ≥96.5%) (trade name: Pripol™ 2033) was obtained from Cargill (Gouda, The Netherlands). Chloroform (≥98.5%) was purchased from Chempur (Piekary Slaskie, Poland) and methanol (≥99.8%) was bought from Stanlab (Lublin, Poland). *Candida Antarctica* lipase B (CAL-B) covalently immobilized on polyacrylate beads (300-500 μm; ≥95%, Fermase CALB™ 10000), with a nominal activity of 10 000 PLU/g (propyl laurate units per gram dry weight) was acquired from Fermenta Biotech Ltd, Mumbai and Enzyme Catalyzed Polymers LLC (Akron, OH, USA). Before use, CAL-B was pre-dried under vacuum for 24h at 40°C and diphenyl ether was stored over 4Å molecular sieves. The rest of the chemicals were used as received.

2.2 CAL-B catalyzed polycondensation of DMFDCA with various diols.

To obtain furan-based copolyesters, a temperature-varied two-step polycondensation reaction in diphenyl ether was performed. Briefly, 2,5-DMFDCA, α,ω-aliphatic linear diol (α,ω-ALD), dilinoleic diol, and diphenyl ether (200 wt% of total monomers) were inserted into a 100 ml round-bottom flask containing pre-dried CAL-B (10 wt% of total monomers). The reaction was

magnetically stirred in an oil bath at 80 °C for 1 h under inert gas flow to get a homogenous mixture. Next, the temperature was raised to 95 °C and the transesterification reaction started, during which the methanol was collected as a by-product (3 h). Further oligomerization was carried out under a pressure of 600 Torr for 21 h. During this step, the mild vacuum was applied to avoid monomer loss due to evaporation and enable monomer conversion into oligomers. Furthermore, a polycondensation reaction was performed at 95 °C under reduced pressure of 2 Torr for 24 h and at 140 °C for the other 48 h.

After the polymerization, chloroform was added to the reaction flask to dissolve the final products and remove the catalyst via normal filtration. The obtained chloroform solution was then concentrated and added dropwise into excess of cold methanol under continuous stirring. The obtained methanol solution with precipitated white polymer product was then filtered, washed three times with cold methanol, collected, and vacuum-dried at 40 °C for 24 h.

2.3 Methods

2.3.1 Nuclear Magnetic Resonance Spectroscopy

^{1}H and ^{13}C NMR spectra were collected on a Bruker spectrometer (800 MHz, 10 s relaxation delay, 128 scans for ^{1}H- and 700 MHz, 10 s relaxation delay, 2048 scans for ^{13}C-NMR). Deuterated chloroform (CDCl$_3$) was used to dissolve furan-based copolyesters.

2.3.2 The Fourier Transform Infrared (FTIR) spectroscopy

FTIR spectra were registered on a Bruker ALPHA spectrometer equipped with an attenuated total reflection (ATR) accessory. The spectra were recorded in a range of 400 – 4000 cm^{-1} and a resolution of 2 cm^{-1}. Samples were vacuum-dried before measurement and 32 scans were performed for each specimen.

2.3.3 Gel Permeation Chromatography (GPC)

The number (M_n) and weight (M_w) averaged molecular weight, as well as dispersity index (Đ) of furan-based copolymers, were determined by gel permeation chromatography (GPC) using an Agilent 1200 modular HPLC series system with a refractive index detector. The system was equipped with two PLgel 5 µm MIXED-C columns (300x7.5 mm). Calibration was conducted on 12 polystyrene standards with masses (M_p) in the range of 474-1800,000 g/mol. Measurements were performed at 35°C. Chloroform (CHCl$_3$) HPLC grade with a flow rate of 0.7 ml/min was used as the mobile phase. The specimens with a concentration of 3 mg/ml were filtered through a PTFE membrane with a 0.2 µm pore size before measurement. Data were recorded using the "ChemStation for LC" program and analyzed using the "ChemStation GPC Data Analysis Software".

2.3.4 X-ray diffraction (XRD)

X-ray diffraction patterns of furan-based polymeric films were collected using an Empyrean PANalytical X-ray diffractometer using Cu K ($\lambda = 0.154$ nm) as the radiation source. In the 2θ range 10–60 with a step size of 0.026. The crystallinity index (X_c') was computed from the XRD profiles from the ratio between the crystalline peaks area (A_c) and the area of total peaks (crystalline and amorphous) (A_t).

2.3.5 Digital holographic microscope

The microstructure of materials was evaluated after spontaneous crystallization using a Lyncée Tec DHM T1000 digital holographic transmission microscope. A Mach-Zehnder interferometer and 666 nm laser diode emitting linear polarized beam with a low illumination power of 200 µm/cm-2 were used to achieve holographic off-axis geometry. Holograms were captured by a CCD camera (1024 x 1024 pixels, 30 fps) with magnification 10x (objective NA = 0.3; FOV = max 660 µm; no immersion). The lateral resolution was 0.1 µm and the axial resolution was below 1 nm. Data were analyzed using the Koala software of Lyncée Tec. Prior to measurement, samples were placed between two microscope slides, heated to about 20 °C above melting temperature, and cooled to room temperature. The samples were a few µm thick between the slides

2.3.6 Thermal properties

Thermal studies were performed using differential scanning calorimetry (DSC). Measurements were performed on a polymer powder sealed in hermetic aluminum pans using a TA Instruments DSC Q2500 Discovery differential scanning calorimeter in the heating-cooling-heating cycles with the standard rate of 10 °C/min. The measurements were conducted over the temperature range of -90 to 200 °C under a nitrogen atmosphere. The glass transition temperatures (T_g) were taken as a midpoint of the transition during a second heating stage. The melting temperature (T_m) and the crystallization temperature (T_c) were verified as the maximum of the endothermic or exothermic peaks at the DSC thermographs, respectively. Furthermore, the enthalpy of melting (ΔH_m) and crystallization (ΔH_c) were established by the integration of the normalized area of the peaks related to a stated transition. The degree of crystallinity (X_c) of the tested materials was estimated as the ratio of the melting enthalpy of copolyesters (ΔH_m) to the melting enthalpy of fully crystalline copolyester ($\Delta H_m°$). For PHF $\Delta H_m° = 135$ J/g, for POF $\Delta H_m° = 180$ J/g, for PDF $\Delta H_m° = 198$ J/g [5]. For PDDF $\Delta H_m° = 232$ J/g this value has been approximated by extrapolation of enthalpy of fusion of 100% crystalline PHF, POF, and PDF polyesters as a function of the number of carbon atoms within diol unit.
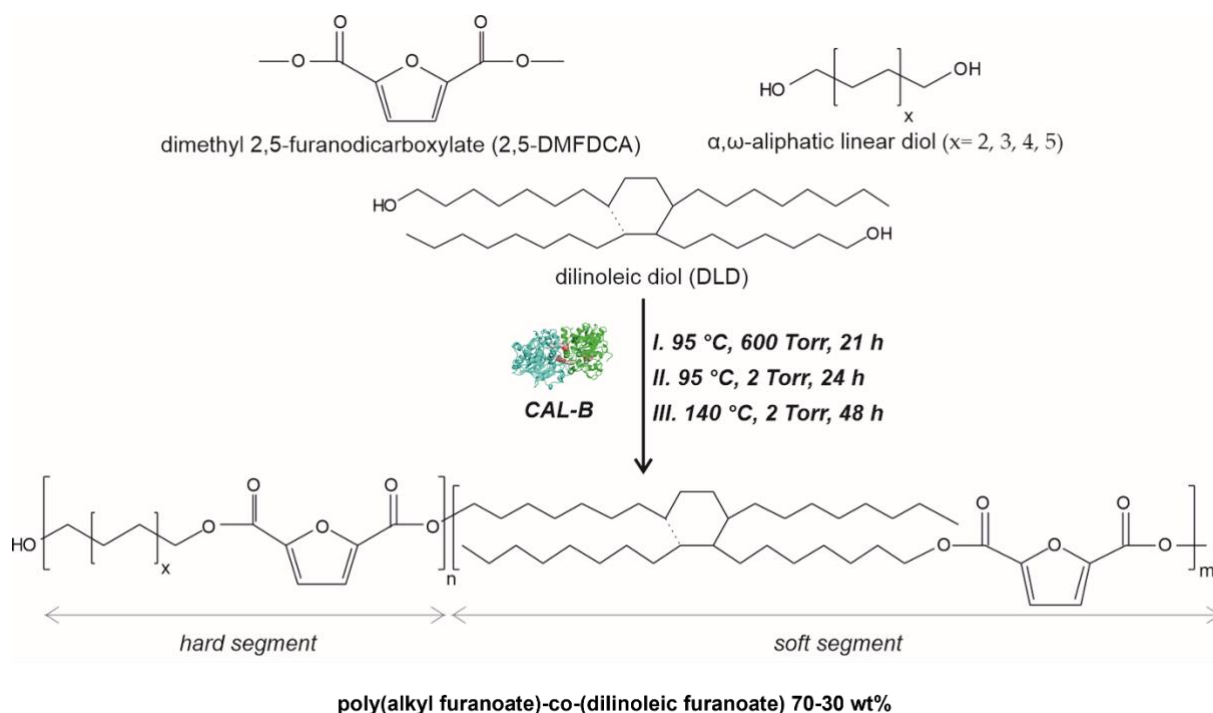
3. Results and discussion

3.1 Enzymatic synthesis and chemical composition of furan-based copolymers

New entirely bio-based series of copolymers containing poly(alkyl furanoate) as a hard segment and poly(dilinoleic furanoate) (DLF) as a soft segment with a 70-30 wt% ratio, respectively, were synthesized in diphenyl ether via direct transesterification of 2,5-DMFDCA with different diols (C = 6, 8, 10, 12 and 36) and consecutive polycondensation via temperature varied two-stage method in diphenyl ether, as illustrated in Scheme 1. As can be concluded from the literature, enzyme catalysts reach the highest catalytic efficiency in temperatures below 100 °C, however, due to the high melting temperatures of furan-based copolyesters and poor solubility of the final products, it was decided to perform the reaction at higher temperature (140 °C). The immobilized form of CAL-B can still maintain its catalytic reactivity in elevated temperatures even up to 150 °C [5,32] which is above the denaturation point of CAL-B protein

which was established experimentally to be 62 °C [33]. On the one hand, this is an advantage because the syntheses can be carried out at higher temperatures, which allows for catalyzing a wide range of reactions, but on the other hand, it should be borne in mind that most probably the depletion of enzyme activity, in this case, is faster which directly translates into the limited reusability. Nevertheless, performed synthesis resulted in four different furan-based copolymers with high reaction yields (> 89 %). The aliphatic diols used to create hard segments were α,ω-aliphatic linear diols (α,ω-ALD) possessing two primary hydroxyl groups: 1,6-HDO, 1,8-ODO, 1,10-DDO, 1,12-DDDO where the number of carbon atoms located between the two hydroxyl groups is 6, 8, 10, and 12, respectively. Dilinoleic diol (1,36-DLD) possessing 36 carbon atoms was used to create the soft segment due to its long aliphatic chain. Depending on the α,ω-ALD used: 1,6-HDO, 1,8-ODO, 1,10-DDO, 1,12-DDDO, copolymers were denoted as PHF-DLF, POF-DLF, PDF-DLF, PDDF-DLF, respectively. Therefore, as the molecular mass and chemical structure of the DLF soft segment were constant, the changes in the composition of the copolymers were consistent with the changes in the hard segments length.

Enzymatic synthesis was also performed using 1,4-butanediol (1,4-BDO), however, due to the poor reaction yield (11 %) and low values of number and weight average molecular weights (1 100 and 1 300 g/mol, respectively), this material was not subjected to further analysis.

dimethyl 2,5-furanodicarboxylate (2,5-DMFDCA)

α,ω-aliphatic linear diol (x= 2, 3, 4, 5)

dilinoleic diol (DLD)

CAL-B

I. 95 °C, 600 Torr, 21 h
II. 95 °C, 2 Torr, 24 h
III. 140 °C, 2 Torr, 48 h

hard segment   soft segment

poly(alkyl furanoate)-co-(dilinoleic furanoate) 70-30 wt%

Scheme 1. General scheme of CAL-B catalyzed synthesis of poly(alkyl furanoate)-co-(dilinoleic furanoate) copolyesters via the temperature-varied two-stage method in diphenyl ether.

3.2 Analysis of the chemical structure of furan-based copolyesters

In order to evaluate the chemical structure of furan-based copolyesters both NMR and FTIR analyzes were performed. Figure 2 depicts the ^{1}H NMR and ^{13}C NMR spectra where the detailed NMR assignments are ascribed as follows:

Poly(hexamethylene furanoate)-co-(dilinoleic furanoate) (PHF-DLF). ^{1}H NMR (800 MHz, CDCl$_3$, ppm): 7.22 (2H, –C$\underline{H}$=, furan ring), 4.35 (4H, –CO–O–C$\underline{H}_2$, from 1,6-HDO and DLD), 3.95 (6H, –O–C$\underline{H}_3$, end group from DMFDCA), 3.69 (4H, –C$\underline{H}_2$–OH, end group from 1,6-HDO and DLD), 1.80 (4H, –CO–O–CH$_2$–C$\underline{H}_2$–, from 1,6-HDO and DLD), 1.49 (1.55 – 1.15 (–C$\underline{H}_2$– internal methylene groups from 1,6-HDO and DLD), 0.88 (6H, –CH$_2$–C$\underline{H}_3$, end groups from DLD); ^{13}C NMR (700 MHz, CDCl$_3$, ppm): 152.88 (–$\underline{C}$=O, furan), 141.67 (=$\underline{C}$–C–O–, furan ring), 113.06 (–C=, furan ring), 60.34 (–CO–O–$\underline{C}$H$_2$–), 57.55 (–$\underline{C}$H$_2$–OH, end group from 1,6-HDO and DLD), 47.13 (–O–$\underline{C}$H$_3$–, end group from DMFDCA), 26.70 – 17.46 (–$\underline{C}$H$_2$–, internal methylene groups from 1,6-HDO and DLD), 8.89 (–CH$_2$–$\underline{C}$H$_3$, end groups from DLD).

Poly(octamethylene furanoate)-co-(dilinoleic furanoate) (POF-DLF). ^{1}H NMR (800 MHz, CDCl$_3$, ppm): 7.19 (2H, –C$\underline{H}$=, furan ring), 4.31 (4H, –CO–O–C$\underline{H}_2$, from 1,8-ODO and DLD), 3.92 (6H, –O–C$\underline{H}_3$, end group from DMFDCA), 3.64 (4H, –C$\underline{H}_2$–OH, end group from 1,8-ODO and DLD), 1.75 (4H, –CO–O–CH$_2$–C$\underline{H}_2$–, from 1,8-ODO and DLD), 1.57 – 1.06 (–C$\underline{H}_2$– internal methylene groups from 1,8-ODO and DLD), 0.86 (6H, –CH$_2$–C$\underline{H}_3$, end groups from DLD); ^{13}C NMR (700 MHz, CDCl$_3$, ppm): 152.92 (–$\underline{C}$=O, furan), 141.71 (=$\underline{C}$–C–O–, furan ring), 112.98 (–C=, furan ring), 60.36 (–CO–O–$\underline{C}$H$_2$–), 57.74 (–$\underline{C}$H$_2$–OH, end group from 1,8-ODO and DLD), 31.90 – 17.45 (–$\underline{C}$H$_2$–, internal methylene groups from 1,8-ODO and DLD), 8.89 (–CH$_2$–$\underline{C}$H$_3$, end groups from DLD).

Poly(decamethylene furanoate)-co-(dilinoleic furanoate) (PDF-DLF). ^{1}H NMR (800 MHz, CDCl$_3$, ppm): 7.19 (2H, –C$\underline{H}$=, furan ring), 4.31 (4H, –CO–O–C$\underline{H}_2$, from 1,10-DDO and DLD), 3.93 (6H, –O–C$\underline{H}_3$, end group from DMFDCA), 3.64 (4H, –C$\underline{H}_2$–OH, end group from 1,10-DDO and DLD), 1.74 (4H, –CO–O–CH$_2$–C$\underline{H}_2$–, from 1,10-DDO and DLD), 1.55 – 1.24 (–C$\underline{H}_2$– internal methylene groups from 1,10-DDO and DLD), 0.87 (6H, –CH$_2$–C$\underline{H}_3$, end groups from DLD); ^{13}C NMR (700 MHz, CDCl$_3$, ppm): 152.94 (–$\underline{C}$=O, furan), 141.73 (=$\underline{C}$–C–O–, furan ring), 112.96 (–C=, furan ring), 60.44 (–CO–O–$\underline{C}$H$_2$–), 57.90 (–$\underline{C}$H$_2$–OH, end group from 1,10-DDO and DLD), 47.18 (–O–$\underline{C}$H$_3$–, end group from DMFDCA), 28.49 – 17.46 (–$\underline{C}$H$_2$–, internal methylene groups from 1,10-DDO and DLD), 8.89 (–CH$_2$–$\underline{C}$H$_3$, end groups from DLD).

Poly(dodecamethylene furanoate)-co-(dilinoleic furanoate) (PDDF-DLF). ^{1}H NMR (800 MHz, CDCl$_3$, ppm): 7.19 (2H, –C$\underline{H}$=, furan ring), 4.32 (4H, –CO–O–C$\underline{H}_2$, from 1,12-DDDO and DLD), 3.93 (6H, –O–C$\underline{H}_3$, end group from DMFDCA), 3.64 (4H, –C$\underline{H}_2$–OH, end group from 1,12-DDDO and DLD), 1.74 (4H, –CO–O–CH$_2$–C$\underline{H}_2$–, from 1,12-DDDO and DLD), 1.40 – 1.25 (–C$\underline{H}_2$– internal methylene groups from 1,12-DDDO and DLD), 0.87 (6H, –CH$_2$–C$\underline{H}_3$, end groups from DLD); ^{13}C NMR (700 MHz, CDCl$_3$, ppm): 152.95 (–$\underline{C}$=O, furan), 141.74 (=$\underline{C}$–C–O–, furan ring), 112.94 (–C=, furan ring), 60.47 (–CO–O–$\underline{C}$H$_2$–), 57.85 (–$\underline{C}$H$_2$–OH, end group from 1,12-DDDO and DLD), 47.14 (–O–$\underline{C}$H$_3$–, end group from DMFDCA), 28.50 – 17.46 (–$\underline{C}$H$_2$–, internal methylene groups from 1,12-DDDO and DLD), 8.89 (–CH$_2$–$\underline{C}$H$_3$, end groups from DLD).
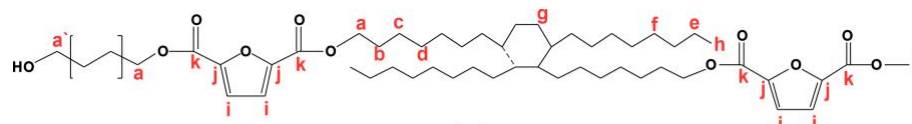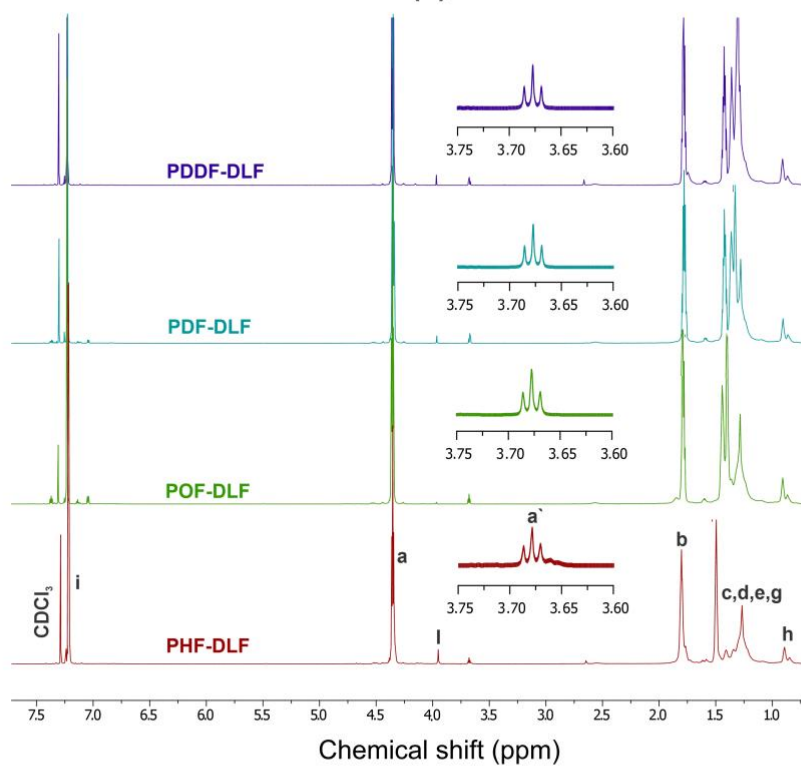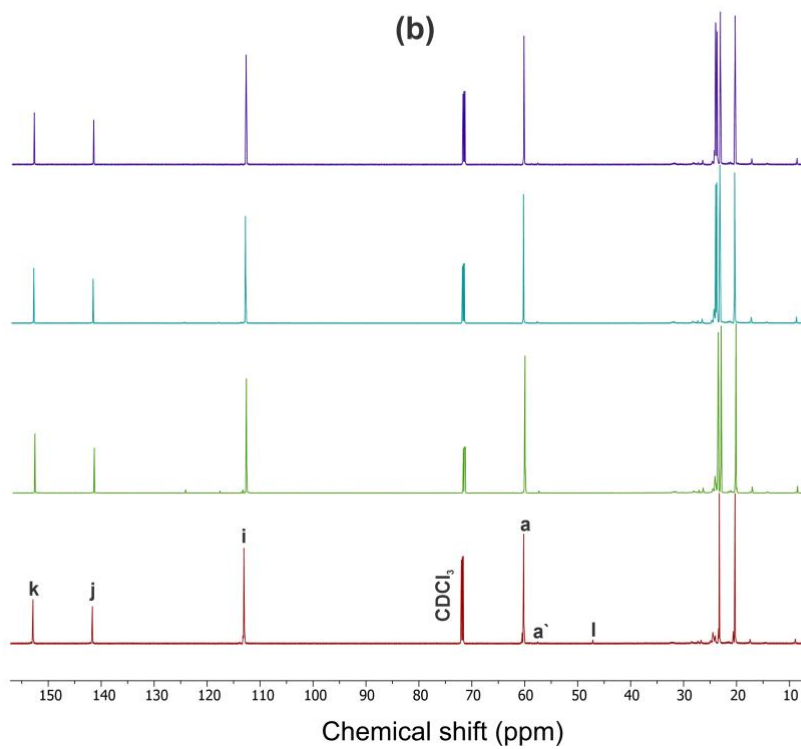
Figure 2. (a) ^{1}H NMR and (b) ^{13}C NMR spectra of the furan-based copolyesters

The collected ^{1}H and ^{13}C NMR spectra verified the chemical structure of copolyesters. Minor signals ascribed to the end-groups of α,ω-ALD appeared at the 3.70 – 3.65 ppm region clearly indicating that enzymatic synthesis was successfully performed and products with relatively high molecular weight were formed. On the basis of the proton signal integration ratio of signals characteristic for hard and soft segments, it was possible to calculate the real segmental composition. Calculated values are close to those established theoretically which indicates good control over the process. However, as can be noticed from Table 1, the content of hard segments increases with an increasing number of carbon atoms within α,ω-ALD. Most probably this phenomenon is related to the fact that under applied vacuum and high reaction temperatures some quantities of diols possessing lower boiling point were removed from the reaction mixture. Since the boiling point values increase with the increasing length of the diol chain, PDDF-DLF material possesses greater hard segment content in comparison to PHF-DLF copolyester (72.1 vs 68.2 wt%, respectively).

The chemical structure of furan-based copolymers was also validated by ATR-FTIR analysis (Fig. 3). The characteristic absorption bands of the obtained furan-based copolyesters are ascribed as follows: ATR-FTIR (cm^{-1}): 3151 and 3118 (=C-H stretching vibrations in the furan ring), 2922 and 2855 (C-H stretching), 1718 (C=O stretching), 1573 and 1506 (C=C stretching vibrations in the furan ring) 1471 and 1390 (-CH- deformations and wagging peaks), 1269 and 1130 (C-O-C asymmetric and symmetric stretchings), 1221 and 1016 (=C-O-C= stretching vibrations in the furan ring), 966, 867, and 764 (C-H bending vibrations in the furan ring).
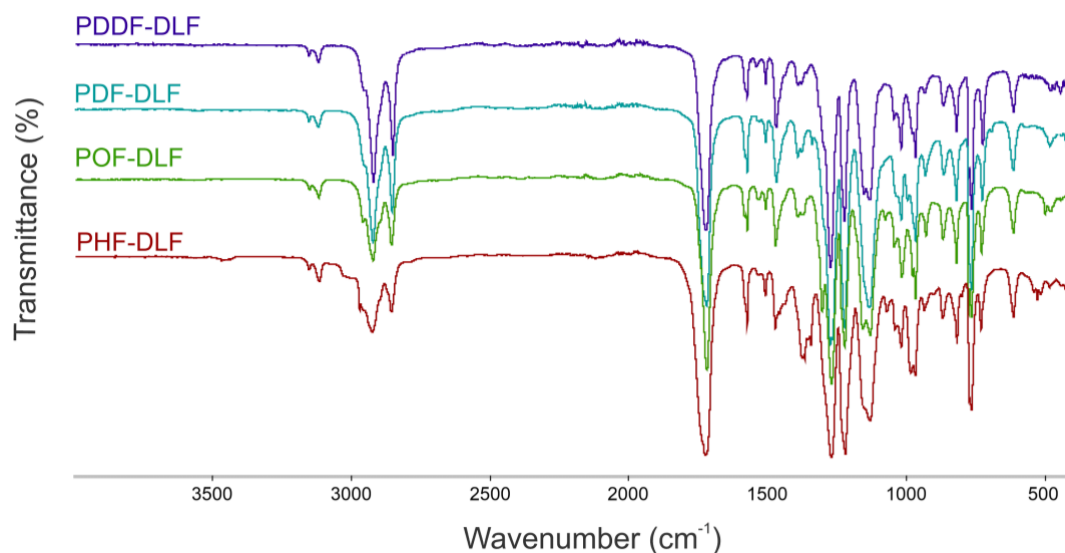
Figure 3. FTIR spectra of furan-based copolyesters.

3.3 The effect of α,ω-aliphatic linear diol chain length on averaged molecular weights of furan-based copolyesters

In order to assess the number (M_n) and weight (M_w) averaged molecular weight of copolyesters GPC analysis was performed. Obtained results revealed that the two-stage enzymatic polymerization of DMFDCA with α,ω-ALD possessing longer chain length yields

furan-based copolyesters with higher molecular weight. This phenomenon is in line with the research conducted by Jiang *et al.* in which they performed a synthesis of furanic-aliphatic polyesters using aliphatic diols differing in chain length and showed that greater M_n and M_w values were achieved for longer-chain α,ω-ALD [5]. As presented in Table 1, molecular weights of copolymers gradually increase with an increasing number of carbon atoms within the α,ω-ALD structure. The M_n and M_w values from 5 700 and 10 700 g/mol increased to 13 700 and 40 500 g/mol, respectively, while changing the number of carbon atoms from 6 to 8. Moreover, further increasing the chain length to 12 enabled to obtain M_n and M_w values of 20 600 and 45 700 g/mol, respectively.

There are two potential explanations for this phenomenon. Firstly, diols with longer alkylene chains have increased enzymatic reactivity, leading to the production of polyesters with higher degrees of polymerization [34]. Secondly, it was proven that the solubility of the furanic-aliphatic polyesters decreases while using α,ω-ALD with shorter chains [5]. Additionally, different melting temperatures (T_m) of copolyesters were noticed. PHF-DLF/POF-DLF materials are characterized by higher T_m (130 and 127 °C, respectively) than that of PDF-DLF/PDDF-DLF materials (96 and 92 °C, respectively) (Table 3), as well as by the synthesis temperature applied during the I and II stage (95 °C). Therefore, during the reaction of DMFDCA with 1,6-HDO/1,8-ODO, low molecular weight products are precipitated from the reaction media due to their high T_m, until the temperature is raised to 140 °C in the final III temperature stage. As a result, polymerization efficiency is lower because CAL-B is unable to reach the polymers most of the reaction time, hence, lower molecular weight values were obtained. On the other hand, enzymatic polymerization of DMFDCA with 1,10-DDO/1,12-DDDO diols which exhibits lower T_m (95 and 91 °C, respectively) proceeded constantly with the same efficiency since no product precipitated out from the reaction media, and the access of CAL-B to polymers was not hindered. As a result, high-molecular-weight copolymers were obtained. Furthermore, focusing on the dispersity index values of furan-based copolyesters they are varying from 1.9 to 3.0 which is typical for polyesters obtained via step-growth polycondensation reactions.

Additionally, based on ^{1}H NMR spectra and integrals of signals corresponding to C$\underline{H}_3$ protons arising from DLD (6H), C$\underline{H}_2$ protons arising from α,ω-ALD diols (4H), and C$\underline{H}_2$-OH protons arising from α,ω-ALD end-groups, number averaged molecular weight (M_n) of copolyesters were calculated following the method described in our previous work [25] and presented in Table 1. Herein, the calculated values differ from those obtained on the GPC basis, however, we are still observing the same trend that M_n values increase with an increasing number of carbon atoms within α,ω-ALD.

Table 1. Composition of furan-based copolyesters determined from ^{1}H NMR and GPC.

Copolymer	Composition		^{1}H NMR[a]	GPC[b]		
	Theoretical wt% [mol%]	Calculated [a] wt% [mol%]	M_n [g/mol]	M_n [g/mol]	M_w [g/mol]	Đ
PHF-DLF	70/30 [86.6/13.4]	68.3/32.7 [85.7/14.3]	17 900	5 700	10 700	1.9
POF-DLF	70/30 [85.3/14.7]	70.7/29.3 [85.3/14.7]	20 500	13 700	40 500	3.0

PDF-DLF	70/30 [84.0/16.0]	71.5/28.5 [85.0/15.0]	21 600	19 000	42 600	2.2
PDDF-DLF	70/30 [82.8/17.2]	72.1/27.9 [84.1/15.9]	27 100	20 600	45 700	2.2

M_n- number average molecular mass, M_w- weight average molecular mass, Đ- dispersity index, [a] values calculated from ^{1}H NMR [b] values determined from GPC.

3.3 The effect of α,ω-aliphatic linear diol chain length on crystalline structure of furan-based copolyesters

In order to evaluate the effects of diol chain length on the crystalline structure of furan-based copolyesters, X-ray diffraction (XRD) analysis was conducted on 100 µm-thick melt-pressed polymer films. Performed studies revealed that furan-based copolyesters are semicrystalline materials. As shown in Figure 3 and Table 2 the diffraction pattern of the tested PHF-DLF was characterized by a low intense peak at 2θ of 13.73 ° ($d = 6.44$ Å) and two strong intense peaks at 2θ of 17.10 ($d = 5.18$ Å) and 24.86 ° ($d = 3.58$ Å). Three similar diffraction peaks can be observed in case of POF-DLF at 12.99 ($d = 6.81$ Å), 16.78 ($d = 5.28$ Å), 24.12 ° ($d = 3.69$ Å) and also in case of PDF-DLF copolymer which XRD patterns appeared at 11.31 ($d = 7.81$ Å), 17.20 ($d = 5.15$ Å), and 23.91 ° ($d = 3.72$ Å). Moreover, for PDDF-DLF copolymer XRD patterns, appeared at 9.74 ($d = 9.08$ Å), 18.14 ($d = 4.88$ Å), and 23.81 ° ($d = 3.73$ Å). According to the presented data and the information provided in the literature [5,35], we assume that the analyzed furan-based copolymers crystallize into β-form crystals, where the three diffraction peaks can be marked as the lattice plan of β(002), β(0 1 0), and β(100), respectively. In case of PDF-DLF and PDDF-DLF intensity of peaks that appeared at region 17.20 (in PDF-DLF) and 18.14 ° (in PDDF-DLF) are getting less pronounced in comparison to PHF-DLF and POF-DLF materials where similar peak appeared in 2θ of 17.10 and 16.78, respectively. This phenomenon suggests that the macromolecular order in PHF-DLF and POF-DLF copolyesters containing shorter diols is higher. Moreover, the rest of the main diffraction peaks mentioned above shifted to lower values when the diol chain length within hard segments increased. As a result, corresponding spacing between the planes in the atomic lattice (d) increased as well, which is quite expected as more space is needed to create the same crystal lattice if the alkylene chain of the diol is longer.

Table 2. XRD analysis of the obtained furan-based copolymers

Copolymer	Crystal type	2θ (°)	d-spacing (Å)	Lattice plane	X_c' (%)
PHF-DLF	Triclinic β -form	13.73	6.44	β(002)	56.5
		17.10	5.18	β(011)	
		24.86	3.58	β(100)	
POF-DLF	Triclinic β -form	12.99	6.81	β(002)	50.0
		16.78	5.28	β(011)	
		24.12	3.69	β(100)	
PDF-DLF	Triclinic β -form	11.31	7.81	β(002)	42.3
		17.20	5.15	β(011)	
		23.91	3.72	β(100)	
PDDF-DLF	Triclinic β -form	9.74	9.08	β(002)	41.1
		18.14	4.88	β(011)	
		23.81	3.73	β(100)	

*d-spacing – spacing between the planes in the atomic lattice*
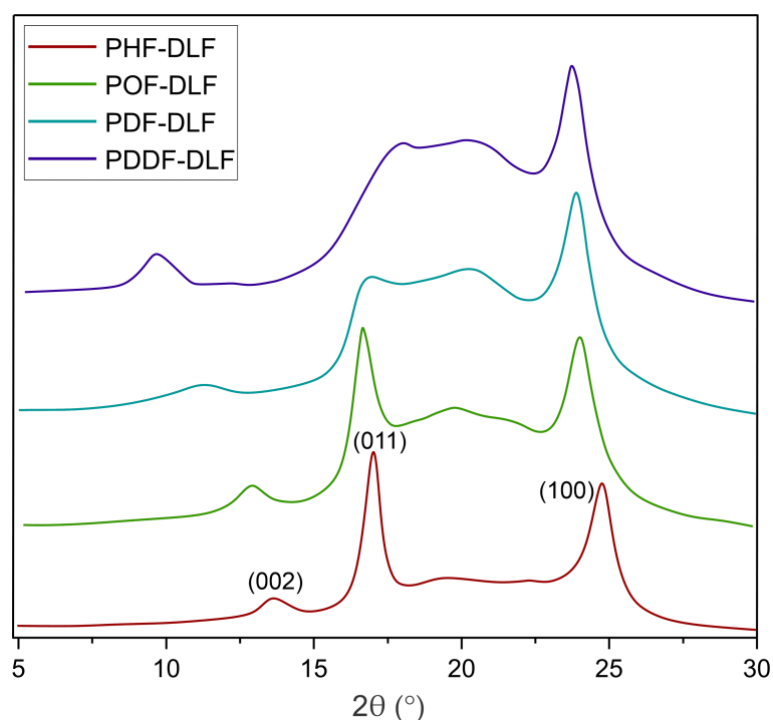
Figure 4. XRD spectra of furan-based copolyesters

Furthermore, the degree of crystallinity (X_c') was calculated from the XRD profiles by the ratio between the crystalline peaks area (A_c) and diffraction area of all peaks (crystalline and amorphous) (A_t) using the following equation (1). The calculated values were collected in Tables 2 and 3, respectively.

$$X_c\text{'} = \frac{A_c}{A_t} \times 100\% \ (1)$$

As shown in Figure 3, the relative area of the amorphous halo increased while changing the number of carbon atoms within α,ω-ALD from 6 to 8, 10, or 12 and as a result, the degree of crystallinity (X_c') decreased. The explanation for this phenomenon is the fact that chain regularity decreases and the ability to form crystal structures is hindered. Additionally, as evident from Figure 4, it also may be correlated with weight averaged molecular mass (M_w). The X_c' values are decreasing with increasing M_w values because the mobility of polymer chains decrease faster with greater M_w, and the entanglement of polymer chains increase quickly in parallel.
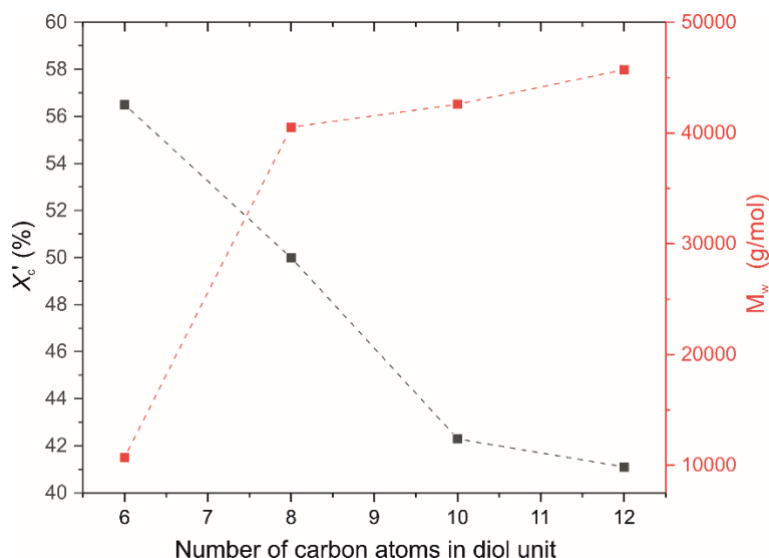
Figure 5. The degree of crystallinity (X_c') and weight average molecular weight (M_w) of furanic-aliphatic polyesters as a function of the number of carbon atoms in α,ω-aliphatic linear diol (α,ω-ALD) unit.

Furthermore, a digital holographic microscope was used to observe and record the crystallization behavior of furan-based copolyesters. Phase images were analyzed, which allow for the measurement of changes in the optical path (refractive index and geometrical path) and density distribution within the sample (Fig 6). By analyzing the profiles along the green lines visible in the phase images, we were able to measure differences in the phase change ($\Delta\varphi$) when the laser beam passed through crystallites versus when it passed through amorphous areas. The images show spherulite formation when the sample of furan-based copolyester was cooled down to room temperature. The red color in Figure 7 corresponds to the greatest phase change of the beam passing through the sample, and the dark blue color corresponds to the least change. The sample thickness was about few micrometers.

The recorded holographic images and profiles along the green lines reveal that the spherulite diameters for furan-based copolymers fall within the range of 4-8 µm (Fig. 8). In most cases, the dimensions of the spherulites within the sample are the same, hence the assumption that the crystallization process probably occurs simultaneously in the entire volume of the sample. Additionally, the phase change between the crystalline and amorphous phase was analyzed and it was observed that the $\Delta\varphi$ values were at least 50% smaller for the PHF-DLF and POF-DLF copolymers (38 and 40 degrees, respectively) in comparison to the PDF-DLF and PDDF-DLF copolymers (80 degrees) (Fig 6). This may indicate that these copolymers have a higher degree of crystallinity or a more homogeneous distribution of crystallites in the amorphous phase, which is in accordance with results obtained from DSC and XRD measurements where a higher degree of crystallinity (X_c and X_c') were recorded for PHF-DLF and POF-DLF copolymers.
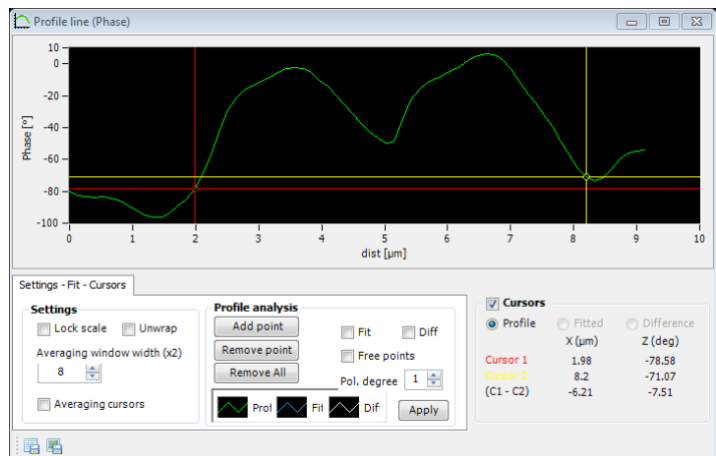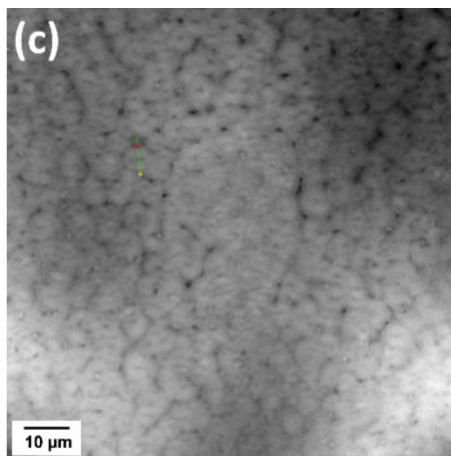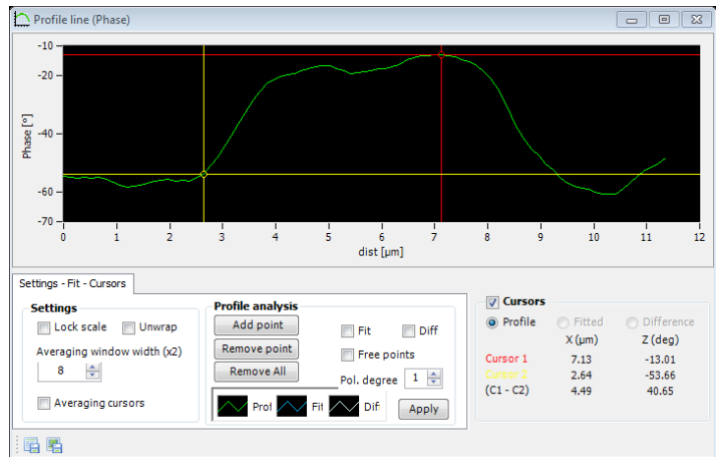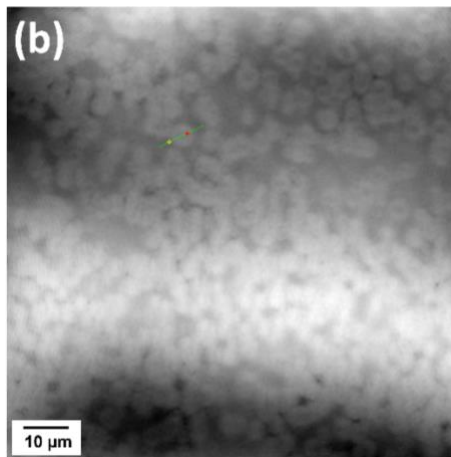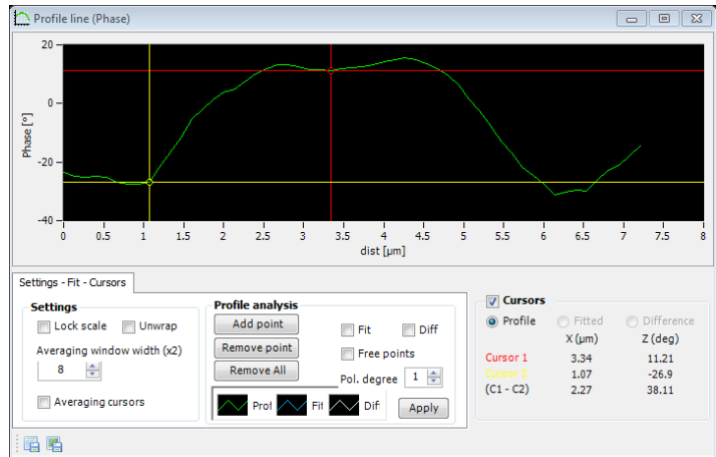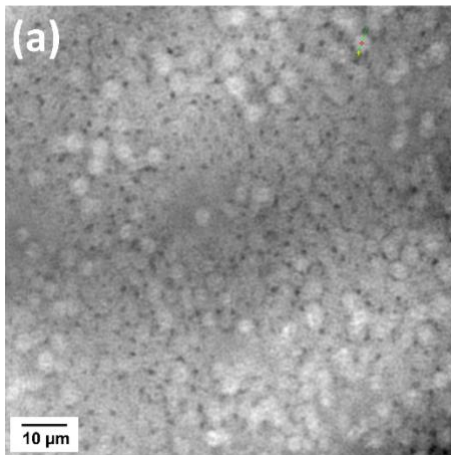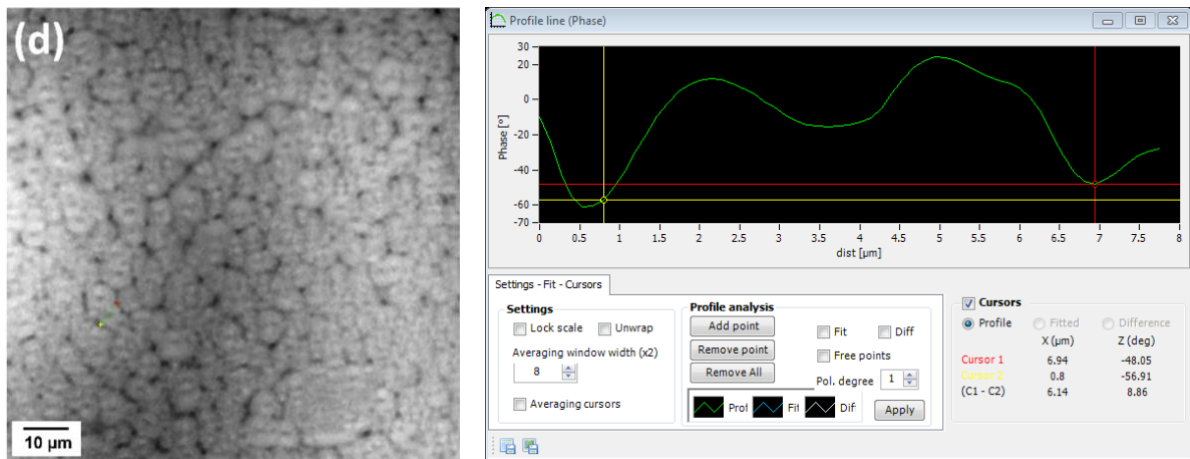
Figure 6. Holographic images and corresponding profiles of the phase changes along the green line recorded for a single spherulite crystallized from the melt for (a) PHF-DLF, (b) POF-DLF, (c) PDF-DLF, (d) PDDF-DLF. The DHM microscope magnification is 50x.

Additionally, it was observed that the density heterogeneity of furan-based copolyesters underwent changes during spontaneous cooling with a decreasing exponentially temperature. The surface roughness parameter (S_a) was calculated to evaluate the degree of homogeneity in the crystallization process. The results, as presented in Figures 7-8, showed that the crystallization process was homogenous throughout the whole volume in the case of the PHF-DLF copolymer, as evidenced by the lowest S_a value. However, as the number of atoms in the diol structure increased, the S_a value also increased, suggesting a less homogenous crystallization process. In particular, the greatest value of Sa was recorded for the PDF-DLF copolymer, indicating that spherulites crystallized at different depths, leading to an increase in the difference of the optical way. These findings indicate that the diol structure has a significant impact on the homogeneity of the crystallization process and have important implications for the design and development of new materials with specific properties. It is also important from a processing point of view since a homogenous crystallization process in polymeric materials can result in a uniform product with consistent properties, while a less homogenous crystallization process can lead to variations in the properties of the final product. Fast crystallization rates can reduce the processing time and allow for the production of materials with improved mechanical and thermal properties. On the other hand, slow crystallization rates can allow for better control over the structure of the crystalline material and may result in materials with improved optical properties. In general, the crystallization rate and the homogeneity of the crystallization process play important roles in the processing of polymeric materials and can influence the final properties of the product.
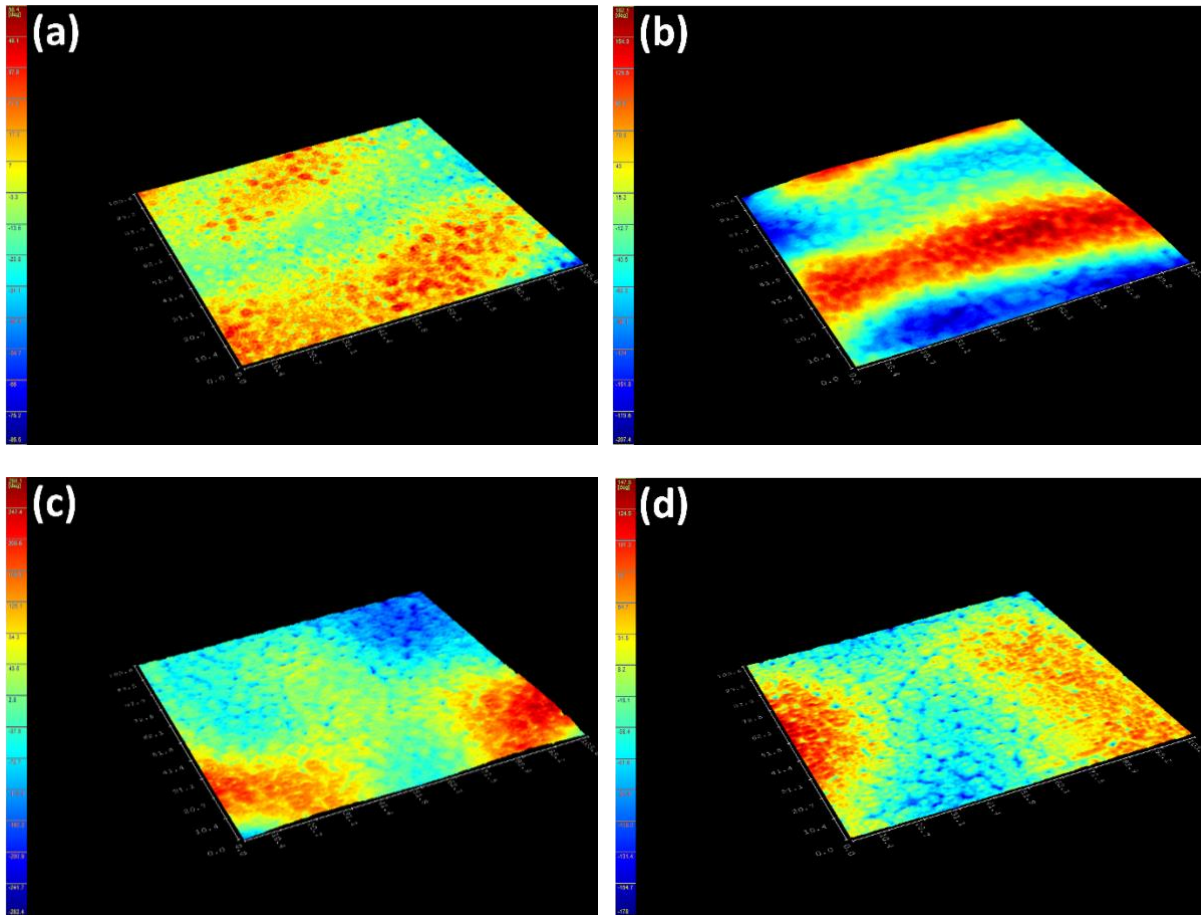
Figure 7. Holographic images of a crystallized layer of (a) PHF-DLF, (b) POF-DLF, (c) PDF-DLF, and (d) PDDF-DLF copolyester.
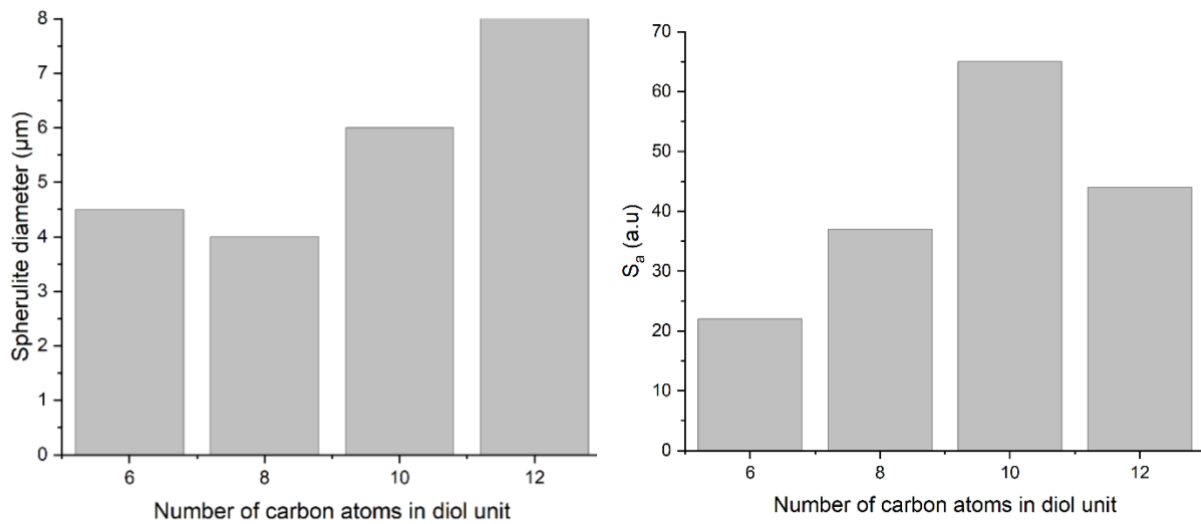
Figure 8. Spherulites diameter (left) and roughness of the sample (S_a) after cooling from melt (right).

3.4 The effect of α,ω-aliphatic linear diol chain length on thermal properties of furan-based copolyesters

DSC analysis has been performed to investigate the relationship between crystalline and thermal effects for furan-based copolyesters consisting of α,ω-ALD differing in the chain length. As can be seen from Figure 9 and Table 3 the thermal transition temperatures are governed by the chain length of α,ω-ALD which were used as a building block to create hard segments within furan-based copolyesters. Performed studies revealed that copolyesters exhibit specific phase-separated microstructure consisting of a crystalline phase, created by the ester hard segments and an amorphous phase formed by a mixture of the soft segments containing long aliphatic dilinoleic diol unit and hard segments which were not involved in crystallites formation. As evident from Figures 9-10 and Table 3 glass transition (T_g), melting (T_m), and crystallization (T_c) temperature as well as crystallization degree (X_c) were observed to decrease steadily with an increasing number of carbon atoms within the α,ω-ALD. This effect can be easily explained since monomers with longer aliphatic chains were introduced to copolyester structure which on the other hand improves material flexibility, as reflected by a decrease of T_g values (from -15 to -21 °C) but on the other, hinders the ability to form crystallites, as reflected by the decrease of X_c and ΔH_m. It is also evident from Figure 9 that the intensity of the crystallization (T_c) and melting (T_m) transition peaks are decreasing and getting broader while changing the number of carbon atoms within α,ω-ALD from 6, 8 to 10, or 12. Moreover, for PDF-DLF and PDDF-DLF copolymers once the glass transition temperature is exceeded during the second heating step, the mobility of macromolecules is gained and further rearrangements take place, as shown by the cold crystallization peak (T_{cc}). This indicates that the crystallization rate of those materials is slower at the tested time scale and that the crystalline phase in this case is less homogenous and crystallites with variable size distribution are formed. This is also in accordance with the conclusions drawn from XRD data that increasing number of carbon atoms within α,ω-ALD hinders crystallization due to the decreasing chain regularity. Of course, herein again, we also cannot neglect the fact, the differences in thermal transitions of PDF-DLF and PDDF-DLF copolyesters can be also influenced by higher values of averaged molecular weights where M_n and M_w are varying from 5 700 to 20 600 g/mol and from 10 700 to 45 700 g/mol, respectively. As was concluded before, it can also affect the crystallization behavior of those copolyesters by reducing the polymer chain mobility. However, similar studies were performed by Loos *et al.* in which they investigated the thermal properties of the 2,5-furandicarboxylic acid-based polyesters that consist of the furan units and α,ω-ALD units possessing different chain lengths (4, 6, 8, and 10 carbon atoms within diol unit). It was found that T_g, T_m, and T_c of 2,5-furandicarboxylic acid-based aliphatic polyesters showed a continuous decrease with an increasing number of carbon atoms within α,ω-ALD from 4 to 10, which is also in agreement with our observations.
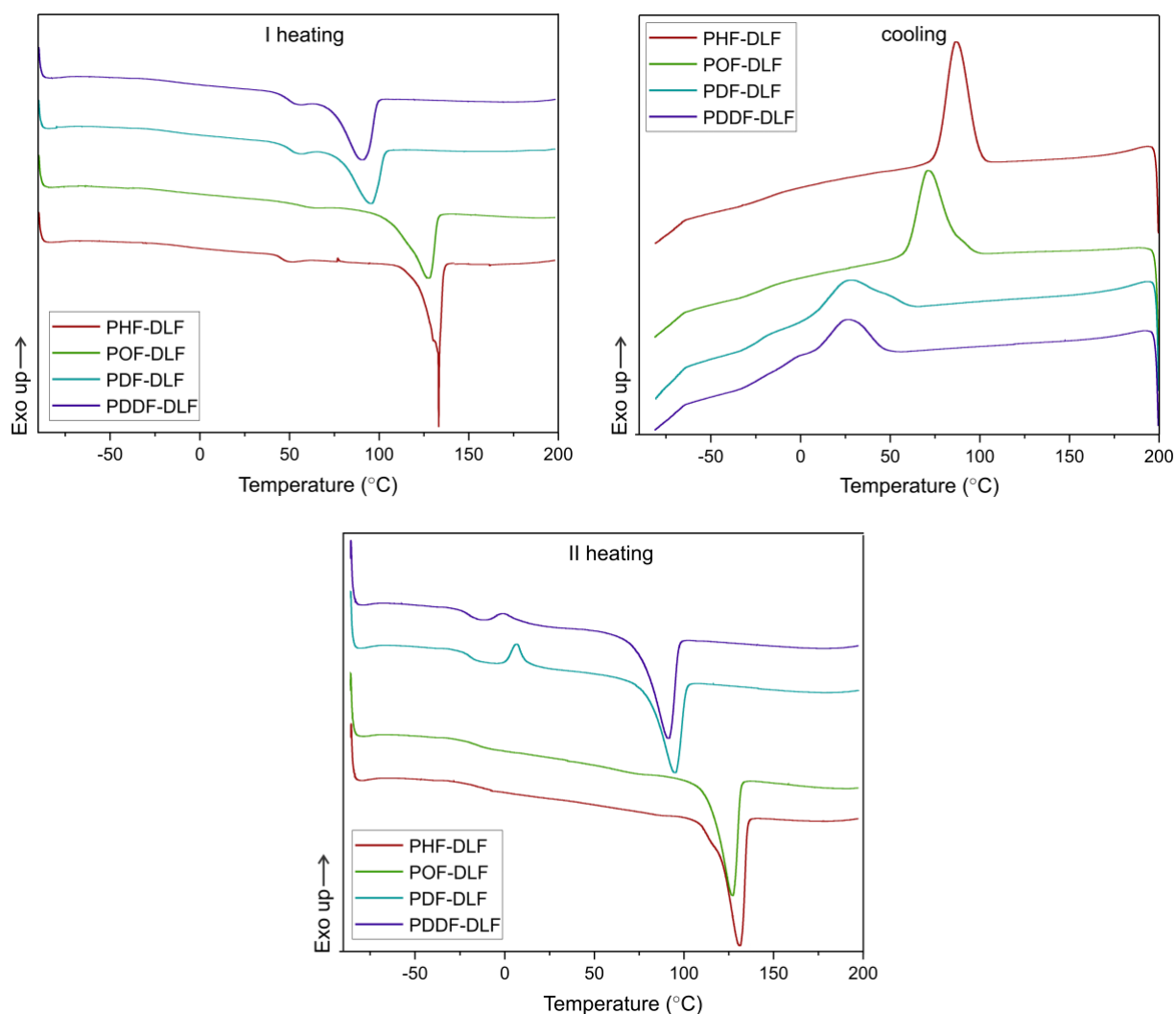
Figure 9. DSC first heating, cooling, and second heating thermograms of furan-based copolymer series.

Table 3. DSC results for furan-based copolymer series

Copolymer	T_g [°C]	ΔC_p [J/g°C]	T_c [°C]	ΔH_c [J/g]	T_{cc} [°C]	ΔH_{cc} [J/g]	T_m [°C]	ΔH_m [J/g]	X_c [%]	X_c ' [%]
PHF-DLF	-15	0.249	87	49.07	-	-	131	41.79	31.0	56.5
POF-DLF	-17	0.266	71	42.36	-	-	127	39.79	22.1	50.0
PDF-DLF	-20	0.348	27	34.14	7	4.57	95	34.52	17.2	42.3
PDDF-DLF	-21	0.317	26	30.33	-1	1.61	91	38.87	13.1	41.1

T_g- glass transition temperature; ΔC_p – heat capacity at T_g; ΔH_m- melting enthalpy; T_m- melting temperature; T_c -crystallization temperature; ΔH_c- crystallization enthalpy; T_{cc} -cold crystallization temperature; ΔH_{cc}- cold crystallization enthalpy X_c- total crystalline phase content in the polymer calculated from DSC. X_c' – total crystalline phase content in the polymer calculated from XRD.
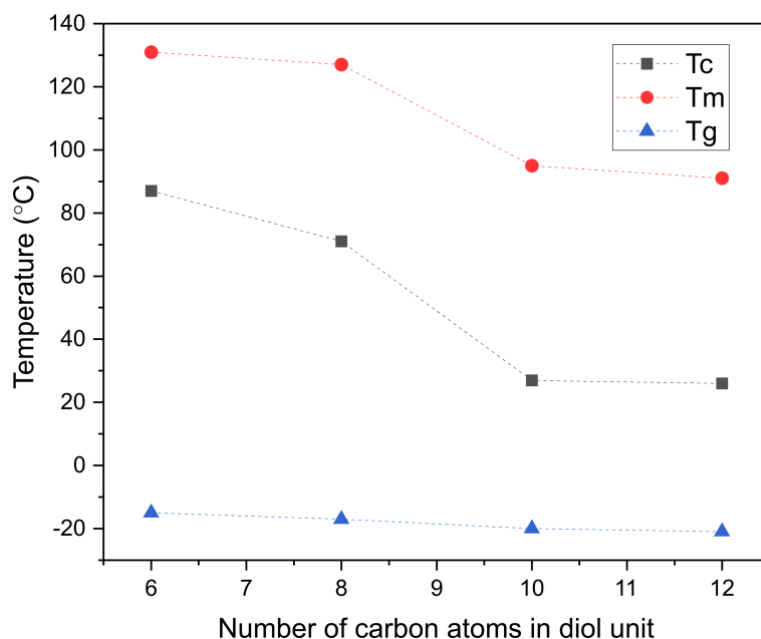
Figure 10. The crystallization (T_c), melting (T_m), and glass transition temperature (T_g) of furan-based copolyesters as a function of the number of carbon atoms in α,ω-aliphatic linear diol (α,ω-ALD) unit.

4. Conclusions

In this study, a new series of entirely bio-based copolymers containing poly(alkyl furanoate) as a hard segment and poly(dilinoleic furanoate) (DLF) as a soft segment with a 70-30 wt% ratio, respectively, were synthesized via an enzymatic process in diphenyl ether. The use of immobilized for of enzyme allowed to perform the synthesis at relatively high temperature (140 °C) enforced by the high melting temperatures of the furan-based copolyesters and poor solubility of the final products. The synthesis resulted in four different furan-based copolymers with high reaction yields (> 89 %).

GPC analysis revealed that using longer chain length α,ω-ALD in the polymerization process led to copolymers with higher molecular weights. This was attributed to increased enzymatic reactivity and decreased solubility of the resulting polyesters with shorter chain length α,ω-ALD. Additionally, the study also revealed that the melting temperatures of the copolymers were affected by the chain length of the α,ω-ALD used in the synthesis, with longer chain length leading to higher melting temperatures. These findings highlight the importance of considering the properties of the starting materials in the enzymatic synthesis of bio-based copolymers.

Furthermore, the chemical structure of the copolymers was evaluated using ^{1}H and ^{13}C NMR spectroscopy, which confirmed that the copolyesters had the expected chemical structure. Additionally, the segmental composition of the copolyesters was calculated and found to be similar to theoretical values, indicating good control over the synthesis process. The content of hard segments in the copolyesters was also observed to increase with an increasing number of carbon atoms in the α,ω-ALD. This is likely due to the removal of diols with lower boiling points from the reaction mixture under the applied vacuum and high temperatures. Furthermore, the number averaged molecular weight of the copolyesters calculated from ^{1}H NMR increased with an increasing number of carbon atoms in the α,ω-ALD.

X-ray diffraction analysis revealed that the furan-based copolyesters are semicrystalline materials and they crystallize into β-form crystals. The study found that the diol chain length within the hard segments had an effect on the crystalline structure of the copolyesters. As the chain length increased, the spacing between the planes in the atomic lattice (d) also increased. Additionally, the degree of crystallinity (Xc') decreased as the number of carbon atoms within α,ω-ALD increased. This is likely due to the decrease in chain regularity and greater capacity of rotational motions of polymer chains which may hinder the ability to form crystal structures.

The study also investigated the behavior of furan-based copolyesters during crystallization using holographic imaging and profiling. The results showed that the spherulite diameters fall within the range of 4-7 µm and the phase change between the crystalline and amorphous phase was smaller for certain copolymers, indicating a higher degree of crystallinity or more homogeneous distribution of the amorphous phase. The diol structure was also found to have a significant impact on the homogeneity of the crystallization process, with increasing S_a values as the number of atoms in the diol structure increases.

In summary, this research has successfully synthesized new bio-based copolymers and demonstrated the significant impact of the characteristics of the starting materials on the enzymatic synthesis process. The study sheds light on the relationship between diol chain length and the crystalline structure of the copolymers, providing valuable information for optimizing the properties of these materials for industrial use. The use of enzymes and monomers derived from biomass in the synthesis of bio-based copolymers is a significant step towards resource-efficiency optimization. By utilizing renewable resources, this process reduces dependence on non-renewable petroleum-based materials and supports sustainability efforts. Furthermore, the development of bio-based copolymers has the potential to reduce greenhouse gas emissions, as the production of biomass-derived materials generates lower emissions compared to traditional petrochemical processes.

In conclusion, this research has a significant contribution to the field of resource-efficiency optimization, as it presents a step towards the development of more sustainable materials which may be useful for various industrial applications.

CRediT authorship contribution statement

Martyna Sokołowska: Methodology, Investigation, Validation, Formal analysis, Writing – original draft, Visualization. **Jagoda Nowak-Grzebyta:** Methodology, Validation. **Ewa Stachowska:** Methodology, Validation, **Piotr Miądlicki:** Methodology. **Beata Michalkiewicz:** Methodology. **Miroslawa El Fray:** Conceptualization, Formal analysis, Supervision, Writing – review & editing, Project administration.

Declaration of Competing Interest

The authors declare that they have no known competing financial interests or personal relationships that could have appeared to influence the work reported in this paper.

Data availability

Data are available upon request

References

[1]   A.J.J.E. Eerhart, A.P.C. Faaij, M.K. Patel, Replacing fossil based PET with biobased PEF; process analysis, energy and GHG balance, Energy Environ Sci. 5 (2012) 6407. https://doi.org/10.1039/c2ee02480b.

[2]   S. Abdolmohammadi, D. Gansebom, S. Goyal, T.-H. Lee, B. Kuehl, M.J. Forrester, F.-Y. Lin, N. Hernández, B.H. Shanks, J.-P. Tessonnier, E.W. Cochran, Analysis of the Amorphous and Interphase Influence of Comononomer Loading on Polymer Properties toward Forwarding Bioadvantaged Copolyamides, Macromolecules. 54 (2021) 7910–7924. https://doi.org/10.1021/acs.macromol.1c00651.

[3]   W. Zhou, Y. Zhang, Y. Xu, P. Wang, L. Gao, W. Zhang, J. Ji, Synthesis and characterization of bio-based poly(butylene furandicarboxylate)-b-poly(tetramethylene glycol) copolymers, Polym Degrad Stab. 109 (2014) 21–26. https://doi.org/10.1016/j.polymdegradstab.2014.06.018.

[4]   J. Zhu, J. Cai, W. Xie, P.-H. Chen, M. Gazzano, M. Scandola, R.A. Gross, Poly(butylene 2,5-furan dicarboxylate), a Biobased Alternative to PBT: Synthesis, Physical Properties, and Crystal Structure, Macromolecules. 46 (2013) 796–804. https://doi.org/10.1021/ma3023298.

[5]   Y. Jiang, A.J.J. Woortman, G.O.R. Alberda van Ekenstein, K. Loos, A biocatalytic approach towards sustainable furanic–aliphatic polyesters, Polym Chem. 6 (2015) 5198–5211. https://doi.org/10.1039/C5PY00629E.

[6]   M. Kwiatkowska, I. Kowalczyk, K. Kwiatkowski, A. Szymczyk, R. Jędrzejewski, Synthesis and structure – property relationship of biobased poly(butylene 2,5-furanoate) – block – (dimerized fatty acid) copolymers, Polymer (Guildf). 130 (2017) 26–38. https://doi.org/10.1016/j.polymer.2017.10.009.

[7]   J. Ma, Y. Pang, M. Wang, J. Xu, H. Ma, X. Nie, The copolymerization reactivity of diols with 2,5-furandicarboxylic acid for furan-based copolyester materials, J Mater Chem. 22 (2012) 3457. https://doi.org/10.1039/c2jm15457a.

[8]   E. Bianchi, M. Soccio, V. Siracusa, M. Gazzano, S. Thiyagarajan, N. Lotti, Poly(butylene 2,4-furanoate), an Added Member to the Class of Smart Furan-Based Polyesters for Sustainable Packaging: Structural Isomerism as a Key to Tune the Final Properties, ACS Sustain Chem Eng. 9 (2021) 11937–11949. https://doi.org/10.1021/acssuschemeng.1c04104.

[9]   D. Maniar, Y. Jiang, A.J.J. Woortman, J. van Dijken, K. Loos, Furan-Based Copolyesters from Renewable Resources: Enzymatic Synthesis and Properties, ChemSusChem. 12 (2019) 990–999. https://doi.org/10.1002/cssc.201802867.

[10] G.Z. Papageorgiou, V. Tsanaktsis, D.G. Papageorgiou, K. Chrissafis, S. Exarhopoulos, D.N. Bikiaris, Furan-based polyesters from renewable resources: Crystallization and thermal degradation behavior of poly(hexamethylene 2,5-furan-dicarboxylate), Eur Polym J. 67 (2015) 383–396. https://doi.org/10.1016/j.eurpolymj.2014.08.031.

[11] P. Skoczinski, M.K. Espinoza Cangahuala, D. Maniar, R.W. Albach, N. Bittner, K. Loos, Biocatalytic Synthesis of Furan-Based Oligomer Diols with Enhanced End-Group Fidelity, ACS Sustain Chem Eng. 8 (2020) 1068–1086. https://doi.org/10.1021/acssuschemeng.9b05874.

[12] M. Jiang, Q. Liu, Q. Zhang, C. Ye, G. Zhou, A series of furan-aromatic polyesters synthesized via direct esterification method based on renewable resources, J Polym Sci A Polym Chem. 50 (2012) 1026–1036. https://doi.org/10.1002/pola.25859.

[13] Long, Timothy E., and John Scheirs, eds. Modern polyesters: chemistry and technology of polyesters and copolyesters. John Wiley & Sons, 2005., (n.d.).

[14] Deopura, B. L., et al., eds. Polyesters and polyamides. Elsevier, 2008., n.d.

[15] E. de Jong, M. A. Dam, L. Sipos and G.-J. M. Gruter, Furandicarboxylic acid (FDCA), a versatile building block for a very interesting class of polyesters, in Biobased Monomers, Polymers, and Materials, ed. P. B. Smith and R. A. Gross, ACS Symposium Series, (n.d.).

[16] A. Gandini, A.J.D. Silvestre, C.P. Neto, A.F. Sousa, M. Gomes, The furan counterpart of poly(ethylene terephthalate): An alternative material based on renewable resources, J Polym Sci A Polym Chem. 47 (2009) 295–298. https://doi.org/10.1002/pola.23130.

[17] A.F. Sousa, C. Vilela, A.C. Fonseca, M. Matos, C.S.R. Freire, G.-J.M. Gruter, J.F.J. Coelho, A.J.D. Silvestre, Biobased polyesters and other polymers from 2,5-furandicarboxylic acid: a tribute to furan excellency, Polym Chem. 6 (2015) 5961–5983. https://doi.org/10.1039/C5PY00686D.

[18] G.Z. Papageorgiou, V. Tsanaktsis, D.G. Papageorgiou, S. Exarhopoulos, M. Papageorgiou, D.N. Bikiaris, Evaluation of polyesters from renewable resources as alternatives to the current fossil-based polymers. Phase transitions of poly(butylene 2,5-furan-dicarboxylate), Polymer (Guildf). 55 (2014) 3846–3858. https://doi.org/10.1016/j.polymer.2014.06.025.

[19] R.J.I. Knoop, W. Vogelzang, J. van Haveren, D.S. van Es, High molecular weight poly(ethylene-2,5-furanoate); critical aspects in synthesis and mechanical property determination, J Polym Sci A Polym Chem. 51 (2013) 4191–4199. https://doi.org/10.1002/pola.26833.

[20] C.H.R.M. Wilsens, J.M.G.A. Verhoeven, B.A.J. Noordover, M.R. Hansen, D. Auhl, S. Rastogi, Thermotropic Polyesters from 2,5-Furandicarboxylic Acid and Vanillic Acid: Synthesis, Thermal Properties, Melt Behavior, and Mechanical Performance, Macromolecules. 47 (2014) 3306–3316. https://doi.org/10.1021/ma500433e.

[21] J.E. Puskas, M.Y. Sen, K.S. Seo, Green polymer chemistry using nature's catalysts, enzymes, J Polym Sci A Polym Chem. 47 (2009) 2959–2976. https://doi.org/10.1002/pola.23351.

[22] S. Sen, J. Puskas, Green Polymer Chemistry: Enzyme Catalysis for Polymer Functionalization, Molecules. 20 (2015) 9358–9379. https://doi.org/10.3390/molecules20059358.

[23] K.P. Dhake, P.J. Tambade, R.S. Singhal, B.M. Bhanage, Promiscuous Candida antarctica lipase B-catalyzed synthesis of β-amino esters via aza-Michael addition of amines to acrylates, Tetrahedron Lett. 51 (2010) 4455–4458. https://doi.org/10.1016/j.tetlet.2010.06.089.

[24] Y. Jiang, A.J.J Woortman, G.O.R. Alberda Van Ekenstein, K. Loos, Environmentally benign synthesis of saturated and unsaturated aliphatic polyesters via enzymatic polymerization of biobased monomers derived from renewable resources, Polym Chem. 6 (2015) 5451–5463. https://doi.org/10.1039/c5py00660k.

[25] M. Sokołowska, J. Nowak-Grzebyta, E. Stachowska, M. El Fray, Enzymatic Catalysis in Favor of Blocky Structure and Higher Crystallinity of Poly(Butylene Succinate)-Co-(Dilinoleic Succinate) (PBS-DLS) Copolymers of Variable Segmental Composition, Materials. 15 (2022) 1132. https://doi.org/10.3390/ma15031132.

[26] Y. Jiang, K. Loos, Enzymatic Synthesis of Biobased Polyesters and Polyamides, Polymers (Basel). 8 (2016) 243. https://doi.org/10.3390/polym8070243.

[27] A. Sonseca, A. McClain, J.E. Puskas, M. El Fray, Kinetic studies of biocatalyzed copolyesters of poly(butylene succinate)(PBS)containing fully bio-based dilinoleic diol, Eur Polym J. 116 (2019) 515–525. https://doi.org/10.1016/j.eurpolymj.2019.04.038.

[28] T. Tsujimoto, H. Uyama, S. Kobayashi, Enzymatic Synthesis of Cross-Linkable Polyesters from Renewable Resources, Biomacromolecules. 2 (2001) 29–31. https://doi.org/10.1021/bm000097h.

[29] C. Japu, A. Martínez de Ilarduya, A. Alla, Y. Jiang, K. Loos, S. Muñoz-Guerra, Copolyesters Made from 1,4-Butanediol, Sebacic Acid, and <scp>d</scp> -Glucose by Melt and Enzymatic Polycondensation, Biomacromolecules. 16 (2015) 868–879. https://doi.org/10.1021/bm501771e.

[30] D. Juais, A.F. Naves, C. Li, R.A. Gross, L.H. Catalani, Isosorbide Polyesters from Enzymatic Catalysis, Macromolecules. 43 (2010) 10315–10319. https://doi.org/10.1021/ma1013176.

[31] M. Sokołowska, E. Stachowska, M. Czaplicka, M. El Fray, Effect of enzymatic versus titanium dioxide/silicon dioxide catalyst on crystal structure of 'green' poly[(butylene succinate)- co -(dilinoleic succinate)] copolymers, Polym Int. 70 (2021) 514–526. https://doi.org/10.1002/pi.6104.

[32] M.B. Frampton, P.M. Zelisko, Synthesis of lipase-catalysed silicone-polyesters and silicone-polyamides at elevated temperatures, Chemical Communications. 49 (2013) 9269. https://doi.org/10.1039/c3cc45380d.

[33] S. Patkar, J. Vind, E. Kelstrup, M. W. Christensen, A. Svendsen, K. Birch and O. Kirk, Chem. Phys. Lipids, 1998, 93, 95–101, (n.d.).

[34] A. Pellis, J.W. Comerford, A.J. Maneffa, M.H. Sipponen, J.H. Clark, T.J. Farmer, Elucidating enzymatic polymerisations: Chain-length selectivity of Candida antarctica lipase B towards various aliphatic diols and dicarboxylic acid diesters, Eur Polym J. 106 (2018) 79–84. https://doi.org/10.1016/j.eurpolymj.2018.07.009.

[35] M. Tasaki, H. Yamamoto, T. Yoshioka, M. Hanesaka, T.H. Ninh, K. Tashiro, H.J. Jeon, K.B. Choi, H.S. Jeong, H.H. Song, M.H. Ree, Crystal structure analyses of arylate polyesters with long methylene segments and their model compounds on the basis of 2-

D X-ray diffractions and infrared progression bands, Polymer (Guildf). 55 (2014) 1228–1248. https://doi.org/10.1016/j.polymer.2014.01.024.